Finite-time stability in randomly-driven classical and quantum systems

Denis Makarov

Laboratory of Nonlinear Dynamical Systems,
V.I. Il'ichev Pacific Oceanological Institute of the Far-East Branch
of the Russian Academy of Sciences,
Vladivostok, Russia

February 27, 2018

Valentin Afraimovich

21.04.1948 – 21.02.2018

The problem

Consider a low-dimensional Hamiltonian system subjected to a weak noisy perturbation. A particular example is a driven one-dimensional nonlinear oscillator with

$$\frac{dq}{dt} = \frac{p}{M}, \quad \frac{dp}{dt} = -\frac{dU}{dq} - \varepsilon\frac{dV}{dq}\xi(t), \quad \varepsilon \ll 1, \tag{1}$$

where M is mass, q is position, p is momentum, $U(q)$ is an unperturbed potential allowing for finite motion, $V(q)$ is a smooth function, $\xi(t)$ is noise with

$$<\xi>= 0, \quad <\xi^2>= 1/2. \tag{2}$$

The corresponding Hamiltonian

$$H = H_0 + \varepsilon H_1(t) = \frac{p^2}{2M} + U(q) + \varepsilon V(q)\xi(t), \tag{3}$$

Under noisy driving, all trajectories are unstable in the Lyapunov sense as $t \to \infty$.

What about finite temporal intervals? How rapidly stability is destroyed?

Why finite-time stability is important for physics?

Trivial answers:

- noise is ubiquitous in nature;
- finite timescales are relevant for physics.

A little bit less trivial:
Regular motion, even under random forcing, is qualitatively different from chaotic motion:

- no heating – energy variations are bounded;
- coherence of close trajectories – meaningful for semiclassical description of quantum dynamics.

Alternating sequence of regular and chaotic regimes gives rise to intermittency and memory effects: essentially non-markovian behavior!

The action-angle variables:

$$I = \frac{1}{2\pi} \oint p\, dq, \quad \vartheta = \frac{\partial}{\partial I} \int\limits_{q'}^{q} p\, dq, \tag{4}$$

$$H = H_0(I) + \varepsilon V(I, \vartheta)\xi(t). \tag{5}$$

The equations of motion in terms of the canonical action-angle variables take form

$$\frac{dI}{dt} = -\frac{\partial H}{\partial \vartheta} = -\varepsilon \frac{\partial V}{\partial \vartheta}\xi(t), \quad \frac{d\vartheta}{dt} = \frac{\partial H}{\partial I} = \omega + \varepsilon \frac{\partial V}{\partial I}\xi(t), \tag{6}$$

where ω is the frequency of unperturbed oscillations.

Let's treat ξ as an unknown but deterministic multifrequency oscillating function.

Consider a finite time interval:

$$0 \leq t \leq \tau.$$

Functions $V(I, \vartheta)$ and $\xi(t)$ can be decomposed in the Fourier series

$$V = \sum_{l=-\infty}^{\infty} V_l \exp[i(l\vartheta + \phi_l)], \quad \xi = \sum_{m=-\infty}^{\infty} \xi_m \exp[i(m\Omega t + \psi_m)], \tag{7}$$

where $\Omega = 2\pi/\tau$. If $V(I, \vartheta)$ is an analytical function, its Fourier-amplitudes decay as $V_l(I) \sim \exp[-\sigma(I)l]$, where σ is the minimal distance between a singularity of $V(\vartheta)$ in the complex plane and the real axis. The Fourier-amplitudes for the function $\xi(t)$ decay as $\xi_m \sim m^{-\beta}$.

Equations of motion can be now rewritten as follows

$$\frac{dI}{dt} = -\frac{i\varepsilon}{2}\sum_{l,m=-\infty}^{\infty} lV_l \xi_m e^{i\Phi_{l,m}}, \quad \frac{d\vartheta}{dt} = \omega + \frac{\varepsilon}{2}\sum_{l,m=-\infty}^{\infty} \frac{\partial V_l}{\partial I}\xi_m e^{i\Phi_{l,m}}, \tag{8}$$

where $\Phi_{l,m} = l\vartheta - m\Omega t + \phi_l - \psi_m$. The stationary phase condition $d\Psi/dt = 0$ implies the resonances

$$mT(I = I_{\text{res}}^{l,m}) = l\tau, \tag{9}$$

where $T(I) = 2\pi/\omega(I)$ is the period of unperturbed oscillations.
The relation $l : m$ defines the order of the respective resonance. It should be noted that an infinite number of resonances $kl : km$ ($k = 1, 2, 3 \ldots \infty$) corresponds simultaneously to each resonant action: the multiresonance.
However, if $I_{\text{res}}^{l,m}$ is far enough from the separatrix value, the product $V_{kl}\xi_{km}$ decreases rapidly with increasing k and only the resonances with small l and m can significantly affect trajectories.
Thus, if $\tau > T(I_{\text{res}}^{l,m})$, only the superior term with $l = 1$ should be taken into account in the equations (8).

Let's consider motion in the neighbourhood of an individual resonance action

$$\Delta I = I - I_{\text{res}}^{l,m}. \tag{10}$$

Now equations of motion look as

$$\begin{gathered} \frac{d(\Delta I)}{dt} = \varepsilon \sum_{k=1}^{K} k l V_{kl} \xi_{km} \sin k\Phi_{kl,km} = -\frac{\partial \tilde{H}}{\partial \Psi}, \\ \frac{d\Psi}{dt} = l\omega_I' \Delta I = \frac{\partial \tilde{H}}{\partial (\Delta I)}, \end{gathered} \tag{11}$$

where K is number of dominant resonances, $\omega_I' = d\omega/dI$,

$$\tilde{H} = k\left(\omega_I' \frac{(\Delta I)^2}{2} + \tilde{U}\right). \tag{12}$$

Potential term in (12) reads

$$\tilde{U} = \varepsilon \sum_{k=1}^{K} V_{kl} \xi_{km} \cos k\Phi_{kl,lm}. \tag{13}$$

Maximal value of ΔI on the separatrix is

$$\Delta I_{\max}^{l,m} = 2\sqrt{\frac{\tilde{U}_{\max}}{|\omega_l'|}}. \tag{14}$$

Quantity $\Delta I_{\max}$ is the halfwidth of resonance in the action space. If $K = 1$, $\tilde{U}_{\max} = V_l \xi_m$, and $\tilde{H}$ transforms into the so-called universal Hamiltonian of nonlinear resonance

$$H_u = \frac{1}{2}\left|\omega_l'\right|(\Delta I)^2 + \varepsilon V_l \xi_m \cos\Psi, \tag{15}$$

Transition to chaos is expected if the celebrated Chirikov criterion

$$\frac{\Delta I_{\max}^{l,m}(\tau) + \Delta I_{\max}^{l',m'}(\tau)}{\delta I(\tau)} \geqslant 1. \tag{16}$$

Here δI is the distance in the action space between resonances $l : m$ and $l' : m'$. If the Hamiltonian system is non-degenerate ($\omega_l' \neq 0$) in the vicinity of resonances, and $\omega > \Omega$, then the distance δI is

$$\delta I(\tau) = \frac{2\pi}{\omega_l' \tau}. \tag{17}$$

- $\tau \ll T$ resonances are weak. Dynamics can be reduced to integrable one via the averaging method, except for narrow layers near separatrices;
- $\tau \simeq T$ resonances are strong, partial or complete destruction of stability is expected;
- $\tau \gg T$ resonances are weak, but their density is very high, expecting complete destruction of stability domains. The exception: in the neighbourhood of degenerate tori stability domains can survive on long times!

Important reminding: our analysis is restricted by time interval $[0 : \tau]$!

Condition of finite-time invariance: *if any set in phase space at $t = 0$ transforms to itself at $t = \tau$ without mixing, then it corresponds to an ensemble of trajectories which are stable by Lyapunov within the interval* $[0 : \tau]$.
This condition is too restrictive!! So, only small fraction of actually existing regular domains may satisfy it: we underestimate actual area of finite-time stability.

Geometrical representation of regular domains satisfying the condition of finite-time invariance is provided by the one-step Poincaré map (DM, M. Uleysky, JPA, 2006):

$$p_{i+1} = p(t = \tau;\, p_i, q_i), \quad q_{i+1} = q(t = \tau;\, p_i, q_i), \tag{18}$$

where $p(t = \tau;\, p_i, q_i)$ and $q(t = \tau;\, p_i, q_i)$ are solitons of equations of motion with initial conditions $p(t = 0) = p_i$, $q(t = 0) = q_i$. As it follows from (18), values of p and q calculated at ith step of mapping become initial conditions for the next $(i + 1)$th step. This procedure is equivalent to the common Poincaré map with the Hamiltonian

$$\bar{H} = \frac{p^2}{2M} + U(q) + \varepsilon \tilde{V}(q,\, t), \tag{19}$$

where

$$\tilde{V}(q,\, \bar{t} + n\tau) = V(q,\, \bar{t}), \quad 0 \leqslant \bar{t} \leqslant \tau, \tag{20}$$

n is integer. Function $\tilde{V}(q,\, t)$ is a sequence of identical pieces of $V(q,\, t)$, each piece is of length τ. In this way we replace the original stochastic dynamical system by an a periodically-driven one. It should be emphasized that this replacement is valid because we restrict ourselves by considering dynamics within the interval $[0 : \tau]$ only.

An example: randomly driven nonlinear pendulum

$$H = \frac{p^2}{2} - \cos x + \varepsilon[f(t)\sin x - f(t+\Delta)\cos x], \tag{21}$$

where $f(t)$ is so-called harmonic noise being solution of coupled stochastic differential equations

$$\dot{f} = y, \quad \dot{y} = -\Gamma y - \omega_0^2 f + \sqrt{2\Gamma}\xi(t), \tag{22}$$

where Γ is a positive constant, and $\xi(t)$ is Gaussian white noise. The terms $f(t)$ and $f(t+\Delta)$ correspond to identical realizations of harmonic noise and differ only by the temporal shift Δ. The first two moments of harmonic noise are given by

$$\langle f \rangle = 0, \quad \left\langle f^2 \right\rangle = \frac{1}{\omega_0^2}. \tag{23}$$

In the case of low values of Γ, the power spectrum of harmonic noise has the peak at the frequency

$$\omega_{\mathrm{p}} = \sqrt{\omega_0^2 - \frac{\Gamma^2}{2}}. \tag{24}$$

Width of the peak is given by the formula

$$\Delta\omega = \sqrt{\omega_{\mathrm{p}} + \Gamma\omega'} - \sqrt{\omega_{\mathrm{p}} - \Gamma\omega'}, \quad \omega' = \sqrt{\omega_0^2 - \Gamma^2/4}. \tag{25}$$

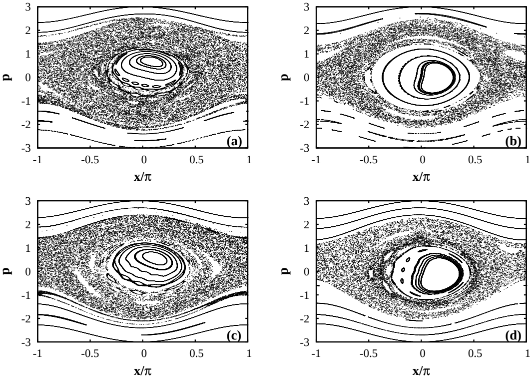

Figure: phase space portraits constructed via one-step Poincaré map with $\tau = 4\pi$. Figures (a)-(d) correspond to different realizations of harmonic noise.

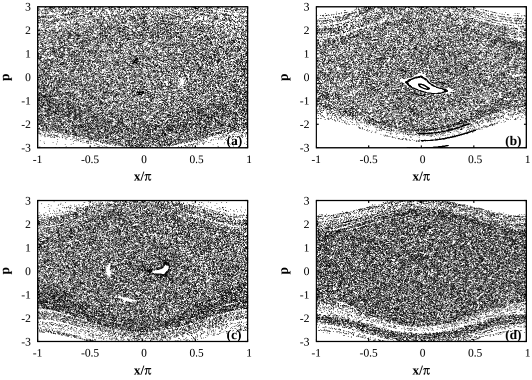

Figure: phase space portraits constructed via one-step Poincaré map with $\tau = 20\pi$. Figures (a)-(d) correspond to different realizations of harmonic noise.

Another example: sound rays in an underwater sound channel

Ray trajectories obey the Hamiltonian equations:

$$\frac{dz}{dr} = \frac{\partial H}{\partial p}, \qquad \frac{dp}{dr} = -\frac{\partial H}{\partial z}, \tag{26}$$

where z is ocean depth, r is range, i.e. horizontal coordinate. r plays the role of a time-like variable!

$$H = -\sqrt{n^2(z,r) - p^2} \simeq H_0 + H_1(r), \tag{27}$$

where $n(z,r) = c_0/c(z,r)$ is the refractive index for sound waves, c_0 is a reference sound speed, $p = \tan\phi$, and ϕ is an angle of ray trajectory with respect to the horizontal plane.

$$H_0 = -1 + \frac{p^2}{2} + \frac{\Delta c(z)}{c_0}, \quad H_1(r) = \varepsilon Y(r) \sum_{n=-N}^{N} X_n \cos[n\pi\chi(z)],, \tag{28}$$

where $\Delta c(z) = c(z) - c_0$ has minimum at some depth called the channel axis, therefore, **ray paths in a channel have form of nonlinear oscillations**. H_1 is small random perturbation, $\chi(z) = e^{-z/B} - e^{-h/B}$, and B is a thermocline depth, $Y(r)$ is a random oscillating function.

Let's remind the Hamiltinian governing dynamics near resonance

$$\tilde{H} = k \left(\omega_I' \frac{(\Delta I)^2}{2} + \varepsilon \sum_{k=1}^{K} V_{kl} \xi_{km} \cos k\Phi_{kl,lm} \right), \tag{29}$$

Presence of depth-dependent oscillations of perturbation results in slower decay of V_{kl} with increasing k. It results in onset of nested resonance chains:

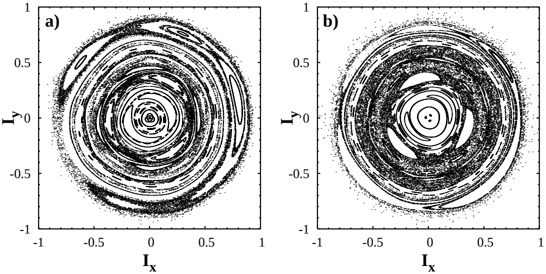

Figure: one-step Poincaré map for sound rays. The polar action-angle variables $I_x = (I/I_s)\cos\theta$ and $I_y = (I/I_s)\sin\theta$ are in units of the separatrix action I_s. Fragments (a) and (b) correspond to two different realizations of noise at the same other conditions (DM, M.Uleysky, M.Budyansky, and S.Prants, PRE 2006).

Ray travel time:

$$TT = \frac{1}{c_0} \int_{r=0}^{R} L \, dr, \quad L = p^2 - H, \tag{30}$$

where L is Lagrangian, R is the distance between the source and the receiving antenna.

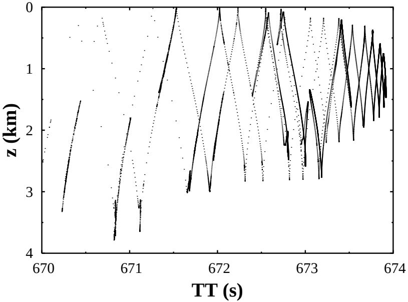

Figure: Timefront at the range 1000 km under the stochastic perturbation: ray arrival depth z vs ray travel time TT. Sharp strips indicate coherent ray clusters originated from phase space domains of stability (DM, M.Uleysky, M.Budyansky, and S.Prants, PRE 2006).

Underwater sound channel in the Sea of Japan

An example of the Hamiltonian system with degenerate tori: $d\omega/dI = 0$ has isolated zeros, corresponding to rays intersecting the channel axis with angle of approximately 1°.

The figure: ray phase space portraits constructed via the one-step Poincaré map. Each column corresponds a single realization of the sound-speed perturbation. Value of the mapping step τ is indicated in the left lower corner of each plot (DM, L. Kon'kov, M. Uleysky, P. Petrov, PRE 2013).

Onset of long-living regular islands in the vicinity of the degenerate tori!

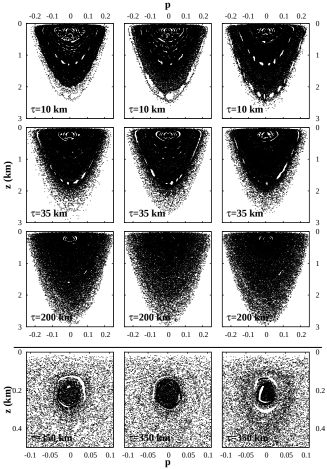

Manifestations of finite-time stability in quantum dynamics

Consider a class of Hamiltonian dynamical systems, where description in terms of classical trajectories corresponds to semiclassical approximation of the related quantum systems. Owing to the principle of quantum-classical correspondence, finite-time stability on the semicalssical level should be reflected in the properties of the quantum dynamics.

Quantum counterpart of one-step Poincaré map is the operator $\hat{G}$ defined as

$$\hat{G}(\tau)\bar{\Psi}(x) = \exp\left(-\frac{i}{\hbar}\hat{H}\tau\right)\bar{\Psi}(x) = \left.\Psi(x,\,t)\right|_{t=\tau}, \tag{31}$$

where $\bar{\Psi}(x) = \Psi(x,\,t=0)$. Hereafter we shall refer to $\hat{G}$ as the finite-time propagator. Peculiarities of classical phase space should be reflected in spectral properties of the finite-time propagator. Eigenvalues and eigenfunctions of the propagator satisfy the equation

$$\hat{G}\Psi_m(x) = g_m\Psi_m(x) = e^{-i\epsilon_m/\hbar}\Psi_m(x). \tag{32}$$

Quantity ϵ_m is the analogue of quasienergy in time-periodic quantum systems. Eigenfunctions Ψ_m can be expanded over eigenstates of the unperturbed potential

$$\Psi_m(x) = \sum_n c_{mn}\phi_n(x). \tag{33}$$

Chaos implies extensive transitions between energy levels, therefore, a chaos-assisted eigenfunction of the propagator should be compound of many unperturbed eigenstates. Thus, one can use the participation ratio

$$\nu = \left(\sum_m |c_{mn}|^4 \right)^{-1}, \tag{34}$$

as measure of “chaoticity”.
An eigenfunction of the finite-time propagator can be projected onto phase space of its classical cointerpart. Phase space region associated with an eigenfunction can be found by means of the parameter

$$\mu = \sum_{m=1}^{M} |c_{mn}|^2 m. \tag{35}$$

Indeed, the formula $\langle I \rangle = \hbar(\mu + 1/2)$ yields the expectation value of the classical action corresponding to the eigenfunction. Parameters ν and μ provide suitable classification of eigenfunctions and can be used for tracking the transition from order to chaos by means of numerical simulation.

Example: randomly-driven quantum pendulum

The Schrödinger equation:

$$i\hbar\frac{\partial\Psi}{\partial t} = -\frac{\hbar^2}{2}\frac{\partial^2\Psi}{\partial x^2} - \cos x + \varepsilon[f(t)\sin x - f(t+\Delta)\cos x]\Psi \tag{36}$$

where $\varepsilon \ll 1$, and $f(t)$ is harmonic noise.

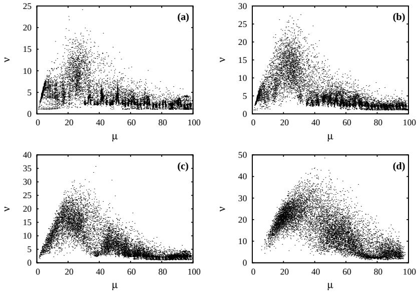

Figure: distribution of FTEO eigenfunctions in the μ-ν plane. Values of τ: (a) 4π, (b) 10π, (c) 20π, (d) 100π (DM, L. Kon'kov, Physica Scripta, 2015).

As domains of finite-time stability in phase space give rise to propagator eigenfunctions with small ν, one can estimate their contribution using the cumulative distribution

$$F(\nu) = \int_1^{\nu} \rho(\nu')\, d\nu', \qquad (37)$$

where $\rho(\nu')$ is the corresponding probability density function.

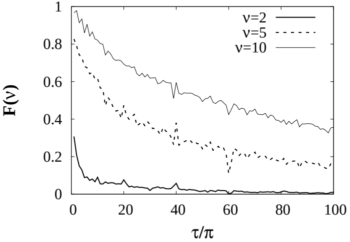

Figure: fractions of eigenfunction ensemble, corresponding to different regimes of localization, vs time.

Sound propagation in an underwater sound channel: full-wave description

Acoustic wavefield is governed by the standard parabolic equation

$$\frac{i}{k_0}\frac{\partial \Phi}{\partial r} = -\frac{1}{2k_0^2}\frac{\partial^2 \Phi}{\partial z^2} + [U(z) + V(z,\, r)]\,\Phi, \tag{38}$$

where wave function Φ is related to acoustic pressure u by means of the formula $u = \Phi \exp(ik_0 r)/\sqrt{r}$. Here the denominator $\sqrt{r}$ responds for the cylindrical spreading of sound. Quantity k_0 is the reference wavenumber related to sound frequency f as $k_0 = 2\pi f/c_0$.

$$U(z) = \frac{\Delta c(z)}{c_0}, \quad V(z,\, r) = \frac{\delta c(z,\, r)}{c_0}. \tag{39}$$

One can easily see that the substitution

$$k_0^{-1} \to \hbar, \quad r \to t \tag{40}$$

transforms the parabolic equation (38) into the Schrödinger equation for a particle with unit mass.

Wave equivalent of the finite-time propagator:

$$\hat{G}(\tau)\bar{\Phi}(z) \equiv \Phi(z,\, r)\big|_{r=\tau}\,. \tag{41}$$

By definition, it describes transformation of a wavefield in course of propagation along a finite waveguide segment of length τ.

Sea of Japan revisited!

Fraction of strongly-localized eigenfunctions as function of distance. The criterion of strong localization is the inequality $\nu \leqslant 2$.

About 5 percents of eigenfunctions remain strongly loczalized for long distances – influence of shearless tori in the classical phase space!

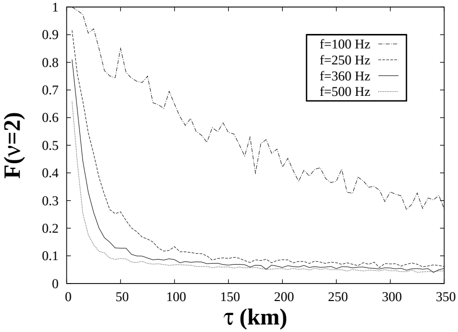

Summary

1. *Phase space domains of finite-time stability can be found via the one-step Poincaré, provided they satisfy the condition of finite-time invariance.*
2. *Formation of such domains of finite-time stability can be described within the theory of deterministic nonlinear resonance.*
3. *Phase space patterns revealed by the one-step Poincaré maps with the same step but different realizations of noise are qualitatively similar.*
4. *Spectral statistics of the quantum one-step propagator contains information about domains of finite-time stability in the classical limit.*

Main publications

- Makarov D.V., Uleysky M.Yu. *Specific Poincaré map for a randomly-perturbed nonlinear oscillator* // Journal of Physics A: Math. Gen., V. 39, P. 489–497 (2006).
- Makarov D.V., Uleysky M.Yu., Budyansky M. V., and Prants S.V. *Clustering in randomly driven Hamiltonian systems* // Physical Review E , V. 73, 066210 (2006).
- Virovlyansky A.L., Makarov D.V., Prants S.V. *Ray and wave chaos in underwater acoustics* // Physics-Uspekhi, V. 55, P. 18–46 (2012).
- Makarov D.V., Kon'kov L.E, Uleysky M.Yu., and Petrov P. S. *Wave chaos in a randomly inhomogeneous waveguide: spectral analysis of the finite-range operator* // Physical Review E , V. 87, 012911 (2013).
- Makarov D.V., Kon'kov L.E. *Order-to-chaos transition in the model of a quantum pendulum subjected to noisy perturbation* // Physica Scripta , V. 90, 035204 (2015).